Study of g-C$_3$N$_4$/BTO composite photocatalyst with ferroelectric polarization under ultrasound

X. G. Ma[a,*], Y. L. Li[a,b], L.G. Cao[b]
aComprehensive test and Analysis Center, North China University of Science and Technology, Tangshan 063210, China
bSchool of materials and Engineering, North China University of Science and Technology, Tangshan 063210, China

Herein, g-C$_3$N$_4$/BTO composite photocatalyst were prepared using melamine, Bi$_2$O$_3$, TiO$_2$, NaCl, and KCl as starting raw materials, and the effect of ferroelectric polarization on photocatalytic properties of g-C$_3$N$_4$/BTO was also investigated. With the increase in the molar percentage of doped BTO samples, the number of square sheet structures has significantly increased, and the tetragonal lamellar structure of BTO samples has further grown, then the wafer size has significantly increased. The degradation performance only degraded less than 20% of RhB under 100 min at the visible light without ultrasound, while, due to the fact that the electric field formed by piezoelectric material is much larger than the defect electric field, which promotes the separation and transmission of carriers, the sample exhibits excellent piezoelectric synergistic photocatalytic effect under ultrasound, especially, g-C$_3$N$_4$/BTO-4 sample   can degrade 88.3% of RhB under ultrasound and light conditions within 30 min, demonstrating the potential and huge application of piezoelectric photocatalytic materials.

1. Introduction

Graphite phase carbon nitride (g-C$_3$N$_4$) is a novel non-metallic polymer that has been used as a photocatalytic material in recent years [1-3]. The advantages of graphite phase carbon nitride (g-C$_3$N$_4$), such as its visible light activity, convenient synthesis of low-cost materials, chemical stability, and unique layered structure, it has attracted the attention of researchers and have been widely studied in various fields. In 2009, X.C. Wang *et al*. [4] first proposed a method that g-C$_3$N$_4$ can decompose water into hydrogen. So far, more and more researchers have studied g-C$_3$N$_4$ as the most promising inorganic non-metallic photocatalyst in the field of photocatalysis, the band gap of g-C$_3$N$_4$ is about 2.7 eV, which is different from TiO$_2$ only activated in the UV spectral region, and it can utilize a larger range of sunlight. However, pure g-C$_3$N$_4$ photocatalysts still suffer from the problems of low separation efficiency, weak redox ability, and low specific surface area of their photogenerated charge carriers, which lead to unsatisfactory photocatalytic activity. Therefore, modifying the surface and Adjusting band gap configuration of the original bulk g-C$_3$N$_4$ can improve its photocatalytic performance [5]. In recent years, many effective methods have been applied to modify the original bulk g-C$_3$N$_4$, such as exfoliation into nanosheets [6], structural defect engineering [7], surface property modification [8], crystal structure optimization [9], nanostructure structure [10], and formation of heterostructures [11].

At present, bismuth based titanates have attracted much attention due to their special structure. The layered structure composed of [Bi$_2$O$_2$]$^{2+}$ layers and polyhedral layers forms an electrostatic field, making them potentially useful in the field of photoelectric conversion. Therefore, bismuth based titanate materials have gradually attracted more and more researchers to study their applications in the field of photocatalysis. Bi$_4$Ti$_3$O$_{12}$ (BTO) is a three-layer bismuth based titanate with promising applications in the field of photocatalysis. In 2003, the

---

photocatalytic activity of $Bi_4Ti_3O_{12}$ was first demonstrated by W.F. Yao *et al*. [12], they used a chemical solution decomposition method to prepare bismuth titanate crystals and applied them to photocatalysis. The results showed that they had a good degradation effect on methyl orange solution. Since then, the application of $Bi_4Ti_3O_{12}$ in the field of photocatalysis has been pioneered. Z.S. Xie *et al*. [13] prepared $Bi_4Ti_3O_{12}$ nanosheets using three methods: molten salt method, solid-state reaction method, and hydrothermal method. The molten salt method $Bi_4Ti_3O_{12}$ exhibits better piezoelectric photocatalytic properties for RhB due to its better shape, crystallinity, and specific surface area. Research has shown that under the combined excitation of light and ultrasound, the shielding effect of the built-in electric field caused by ferroelectric polarization can be broken by the alternating piezoelectric potential caused by periodic mechanical stress, promoting the effective separation and transmission of photogenerated carriers, which greatly improves the photocatalytic performance [14,15]. In this paper, BTO is used to composite with $g-C_3N_4$, and the molar percentages of BTO is 1%, 3%, 7%, 10%, and 15%, respectively. Accordingly the composite photocatalyst named as C_3N_4/BTO-1, C_3N_4/BTO-2, C_3N_4/BTO-3, C_3N_4/BTO-4 and C_3N_4/BTO-5, respectively.

2. Experimental

The melamine powder was ground in a mortar, weighed 10 g, and placed in a crucible, then heated to 550 °C in a muffle furnace in an atmospheric environment, with a heating rate of 5 °C /min, and held for 2 h. After calcination, it was placed in a furnace for cooling, and the yellow powder obtained was pure $g-C_3N_4$. Weighed the raw materials Bi_2O_3, TiO_2, NaCl, and KCl required for the preparation of BTO at 1.28: 5.00: 7.84: 10, respectively. Placed the raw material in a mortar and grind for 1 h. Put the mixed raw materials into a crucible, raised them to 700 °C for 2 h at a speed of 5 °C /min. Took out the sample after it was naturally cooled to room temperature. Added the deionized water and continue grinding to powder. Centrifuged and washed the solution for three times to obtain the lower layer sediment, and dried at 80 °C for 10 h to obtain pure BTO sample. BTO samples were mixed with $g-C_3N_4$ in molar percentages of 1%, 3%, 7%, 10%, and 15%, respectively, filled with alcohol and stirred for 3 h, followed by ultrasonic dispersion for 3 h, then evaporated to obtain a powder, finally, the powder was calcined 550 °C for 2 h to obtain the composite sample $g-C_3N_4$/BTO.

The phase structure of the samples is confirmed by X-ray diffraction (XRD, D/MAX 2500 PC, Rigaku). The morphology is observed by scanning electron microscopy (SEM, scios). The photocatalytic of $g-C_3N_4$/BTO are evaluated by degrading RhB solution under light irradiation (Xe lamp, PLS-SXE300CUV) and ultrasonic vibration (Ultrasonic cleaner, SB-3200).

3. Results and discussions

In order to explore the phase composition of the composite sample, XRD analysis was performed on the sample, and the results are shown in Fi. 1. The five samples can exhibit BTO related peaks, but almost no diffraction peaks related to $g-C_3N_4$ are observed. This is already due to the fact that BTO is a very typical crystal structure with very good crystallinity, while the crystallinity of $g-C_3N_4$ itself is relatively poor, and the diffraction peak intensity of pure samples is not very high, resulting in an inconspicuous diffraction peak of $g-C_3N_4$.
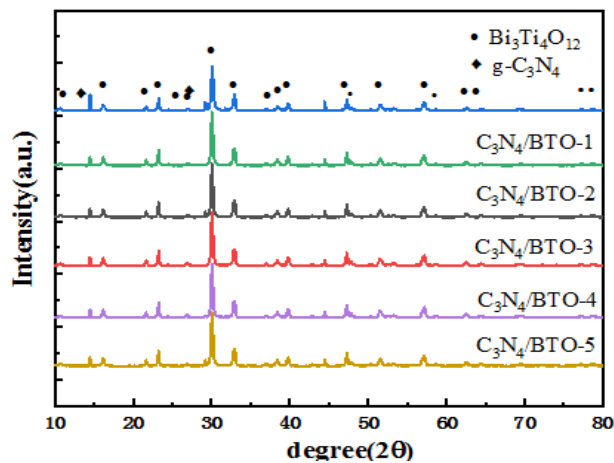
Fig. 1. XRD pattern of the samples.

SEM images of the g-C$_3$N$_4$/BTO composite materials are shown in Fig. 2. In Fig.2, it can be seen that a large amount of amorphous cluster-like material is wrapped around the sporadic square sheet structure, and the square flake structure is a BTO sample.
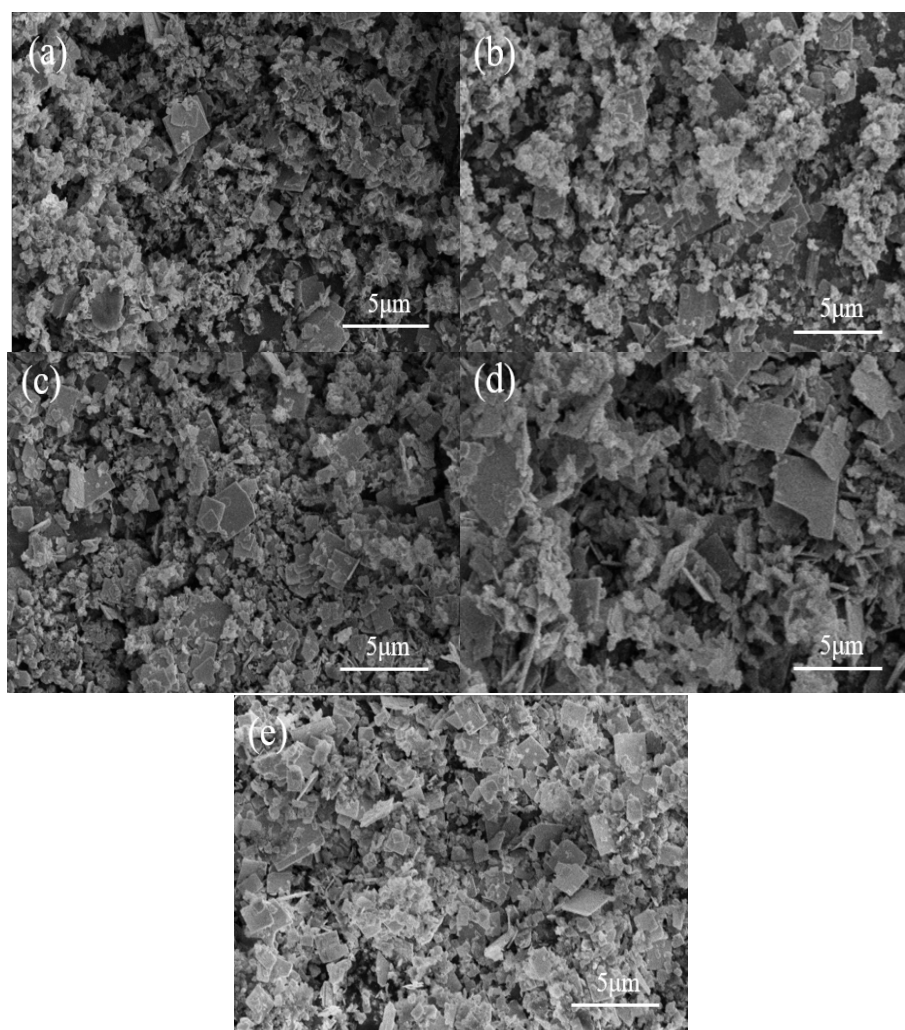

Fig. 2. SEM image of the samples: (a) CN/BTO-1, (b) CN/BTO-2, (c) CN/BTO-3, (d) CN/BTO-4, and (e) CN/BTO-5.
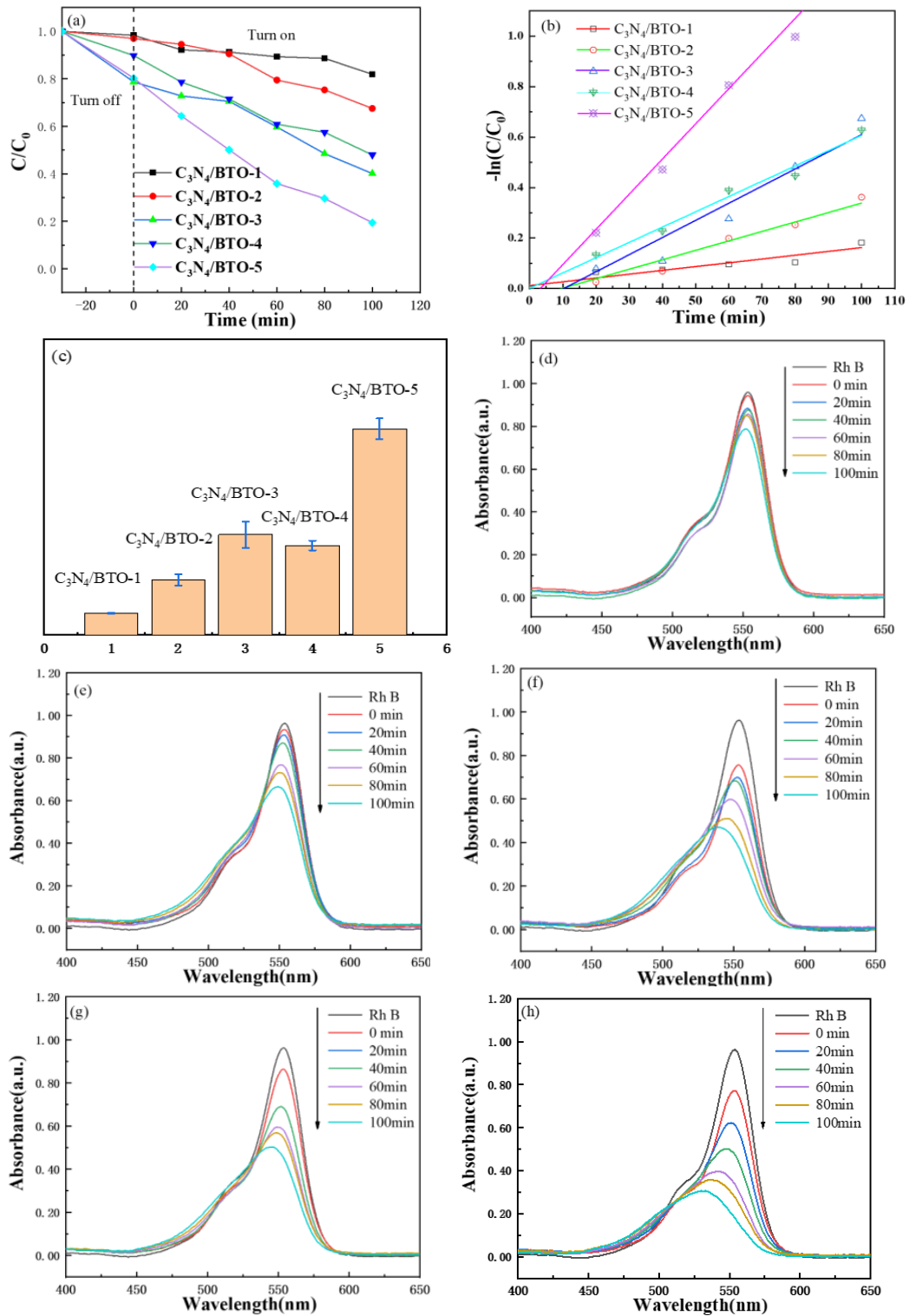
Fig. 3. Analysis of degradation performance of the samples: (a) Degradation curve, (b) kinetic analysis, (c) Kinetic constant, (d) CN/BTO-1, (e) CN/BTO-2, (f) CN/BTO-3, (g) CN/BTO-4, and (h) CN/BTO-5.
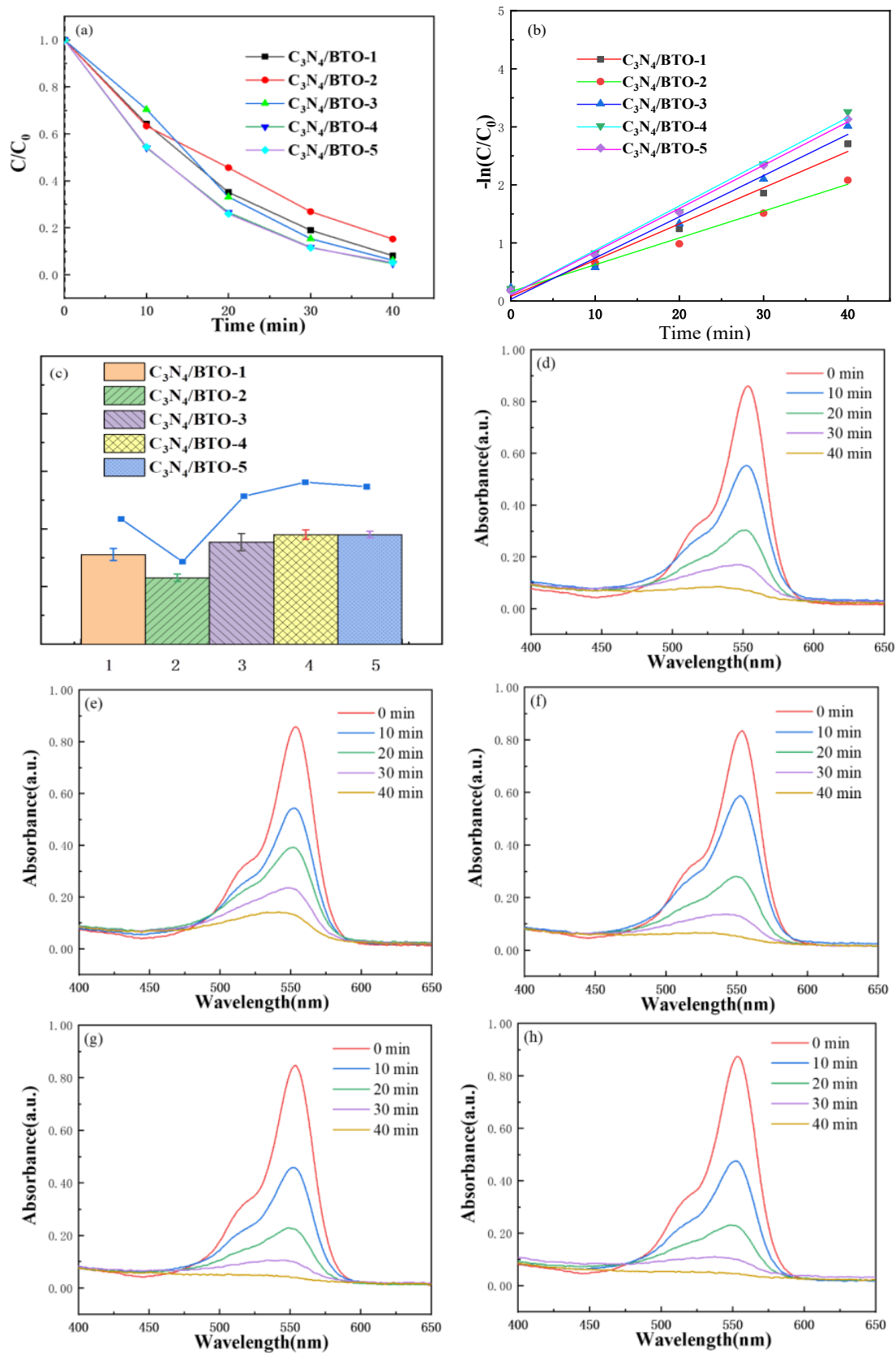
Fig. 4. Analysis of degradation performance of the samples under ultrasound: (a) Degradation curve, (b) kinetic analysis, (c) Kinetic constant, (d) CN/BTO-1, (e) CN/BTO-2, (f) CN/BTO-3, (g) CN/BTO-4, and (h) CN/BTO-5.

The amorphous material is g-C_3N_4 particles peeled off after ultrasound. With the increase in the molar percentage of doped BTO samples, the number of square sheet structures in SEM images of the same size has significantly increased. The tetragonal lamellar structure of BTO samples has further grown, and the wafer size has significantly increased. This is mainly due to the secondary calcination, which increases the holding time of the BTO reaction and promotes the further reaction of BTO, therefore, the grain size development is better.

In order to characterize the change in catalytic performance of the composite sample, a visible light degradation experiment was conducted on the sample, and the results are shown in Fig. 3. In Fig. 3(a), as the doping amount of BTO increases, the adsorption and degradation properties of the sample increase. The adsorption capacity of g-C_3N_4/BTO-1 samples almost disappeared after incorporation of a small amount of BTO, while the degradation performance only degraded less than 20% of RhB in 100 min at the visible light. Fig3. 3(d)-(h) shows the complete degradation spectra of the five samples, an obvious phenomenon is that the maximum absorption peak of the solution has shifted, which is related to the degradation process of RhB. Under photocatalytic conditions, when RhB is degraded, it is first deethylated, and RhB is degraded into an intermediate product, furthermore the maximum absorption peak of the intermediate product is different from RhB, so the maximum absorption peak has shifted. With the further decomposition of the intermediate product, the maximum absorption peak gradually shifts to blue direction.

In order to characterize the piezoelectric synergetic photocatalytic performance of the sample, a piezoelectric synergetic catalytic degradation experiment was conducted on the sample under full sunlight irradiation, and the results are shown in Fig.4. Under the dual effects of light and ultrasound, the overall degradation performance of the sample has significantly improved. In general, the overall piezoelectric co photocatalytic performance of the five samples did not differ significantly, and the degradation was almost completed within 40 min. In the kinetic analysis and kinetic constant change diagram in Fig. 4(b), it can be seen that the best piezoelectric synergistic catalytic degradation effect is g-C_3N_4/BTO-4 sample, which can degrade 88.3% of RhB under ultrasound and light conditions within 30 min. Fig. 4(d)-(h) show the full spectrum of degradation of the five samples, unlike the full spectrum of only photocatalytic degradation, there is no significant shift in the maximum absorption peak of the solution under piezoelectric and photocatalytic condition. Wu et al. [16] believe that in the RhB catalytic process, $\cdot O_2^-$ tends to promote deethylation, while $\cdot OH$ will directly deconstruct the aromatic ring in the molecule, during the photocatalytic process, more $\cdot O_2^-$ is generated, while the amount of $\cdot O_2^-$ and $\cdot OH$ generated by piezoelectric catalysis is relatively balanced, and the dye molecules will further decompose rapidly after deethylation.

The defects of BTO prepared by the molten salt method are relatively high. When the size of the layered BTO increases, the corresponding defects accumulate, when the atoms or electrons are absent at the defect, a small local electric field is formed, which becomes the center of a new photogenerated carrier recombination, as shown in Fig. 5(a). Therefore, when the two-dimensional BTOs containing defects are combined with g-C_3N_4, these defects will also induce the recombination of photogenerated carriers of g-C_3N_4, so the performance of the composite material cann't be improved. In Fig. 5(b) and (c), with the addition of ultrasound, a piezoelectric effect occurs on the surface of the sample, and positive and negative charges accumulate on both sides of the surface. Due to the fact that the electric field formed by piezoelectric material is much larger than the defect electric field, which promotes the separation and transmission of carriers, the sample exhibits excellent piezoelectric synergistic photocatalytic effect.
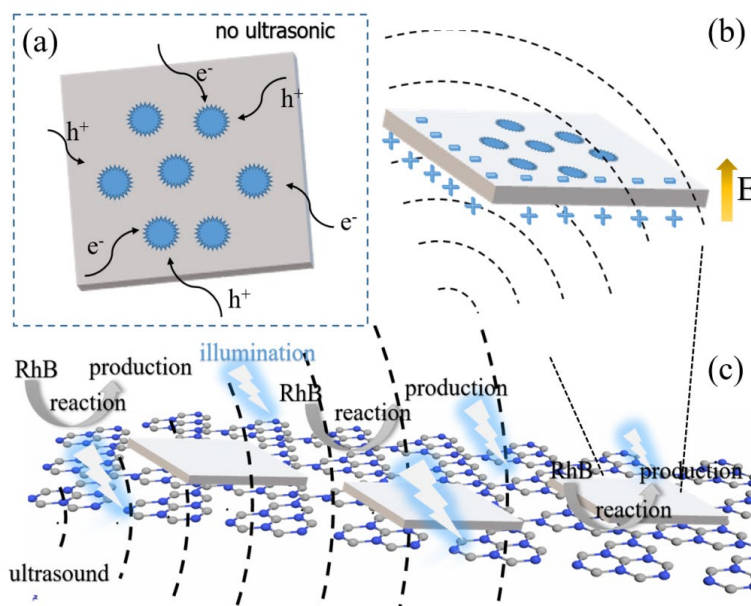
Fig. 5. Schematic diagram of photocatalytic degradation: (a) Without ultrasound, (b) with ultrasound, and (c) degradation diagram.

4. Conclusions

In this scientific research work, g-C_3N_4/BTO composite photocatalyst were prepared, and the effect of ferroelectric polarization on photocatalytic properties of g-C_3N_4/BTO was also investigated. With the increase in the molar percentage of doped BTO, the number of square sheet structures was significantly increased, and the tetragonal lamellar structure of BTO samples was further grown, then the wafer size was significantly increased. The degradation performance only degraded less than 20% of RhB in 100 min at the visible light without ultrasound, and the maximum absorption peak of the solution has shifted, which is related to the degradation process of RhB. In the meanwhile, the overall degradation performance of the sample has significantly improved under the dual effects of light and ultrasound, and there is no significant shift in the maximum absorption peak of the solution under piezoelectric and photocatalytic condition. Thanks to the electric field formed by piezoelectric material, it promotes the separation and transmission of carriers, the sample exhibits excellent piezoelectric synergistic photocatalytic effect under ultrasound, and g-C_3N_4/BTO-4 sample can degrade 88.3% of RhB under ultrasound and light conditions within 30 min. Our research work provides a new strategy for solving the separation and transportation of photogenerated carriers.

References

[1] J.H. Wu, F.Q. Shao, X.Q. Luo, et al, Applied Surface Science 471, 935 (2019); https://doi.org/10.1016/j.apsusc.2018.12.075

[2] L.S. Zhang, N. Ding, L.C. Lou, et al, Advanced Functional Materials 29, 1806774 (2019).

[3] D.M. Zhao, C.L. Dong, B. Wang, et al, Advanced Materials 31, 1903545 (2019)

[4] X.C. Wang, K. Maeda, A Thomas, et al, Nature Materials 8, 76 (2009); https://doi.org/10.1038/nmat2317

[5] F.K. Kessler, Y. Zheng, D. Schwarz, et al, Nature Reviews Materials 2, 17030 (2017); https://doi.org/10.1038/natrevmats.2017.30

[6] J. Xu, L.W. Zhang, R. Shi, et al, Journal of Materials Chemistry A 1, 14766 (2013); https://doi.org/10.1039/c3ta13188b

[7] P.W. Chen, K. Li, Y.X. Yu, et al, Applied Surface Science 392, 608 (2017); https://doi.org/10.1016/j.apsusc.2016.09.086

[8] M.L. Zhang, Y. Yang, X.Q. An, et al, Journal of Hazardous Materials 424, 127424 (2021); https://doi.org/10.1016/j.jhazmat.2021.127424

[9] Z.H. Zhang, L.F. Cui, Y. Zhang, et al, Applied Catalysis B: Environmental 297, 120441 (2021); https://doi.org/10.1016/j.apcatb.2021.120441

[10] D.D. Zheng, C.J. Huang, X.C. Wang, Nanoscale 7, 465 (2015); https://doi.org/10.1039/C4NR06011C

[11] C. Ji, C. Du, J.D. Steinkruger, et al, Materials Letters 240, 128 (2019); https://doi.org/10.1016/j.matlet.2018.12.128

[12] W.F. Yao, H. Wang, X.H. Xu, et al, Materials Letters 57, 1899 (2003); https://doi.org/10.1016/S0167-577X(02)01097-2

[13] Z.S. Xie, X.L. Tang, J.F. Shi, et al, Nano Energy 98, 107247 (2022); https://doi.org/10.1016/j.nanoen.2022.107247

[14] C.L. Liu, J.J. XU, J.F. NIU, et al, Separation and Purification Technology 241, 116622 (2020); https://doi.org/10.1016/j.seppur.2020.116622

[15] H. Sun, Z.R. Xu, X. Xie, et al, Journal of Alloys and Compounds 882, 160609 (2021); https://doi.org/10.1016/j.jallcom.2021.160609

[16] J.R. Wu, W.W. Wang, Y. Tian, et al, Nano Energy 77, 105122 (2020); https://doi.org/10.1016/j.nanoen.2020.105122